

Design of a Structurally Novel Multipotent Drug Candidate by the Scaffold Architecture Technique for ACE-II, NSP15, and M^{PRO} Protein Inhibition: Identification and Isolation of a Natural Product to Prevent the Severity of Future Variants of Covid 19 and a Colorectal Anticancer Drug

Sourav Pakrashy, Prakash K. Mandal, Surya Kanta Dey, Sujata Maiti Choudhury, Fatmah Ali Alasmay, Amani Salem Almalki, Md Ataul Islam, and Malay Dolai*



Cite This: *ACS Omega* 2022, 7, 33408–33422



Read Online

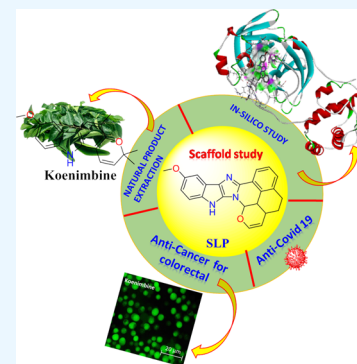
ACCESS |

Metrics & More

Article Recommendations

Supporting Information

ABSTRACT: Scaffold architecture in the sectors of biotechnology and drug discovery research include scaffold hopping and molecular modelling techniques and helps in searching for potential drug candidates containing different core structures using computer-based software, which greatly aids medicinal and pharmaceutical chemistry. Going ahead, the computational method of scaffold architecture is thought to produce new scaffolds, and the method is capable of helping search engines toward producing new scaffolds that are likely to represent potent compounds with high therapeutic applications, which is a possibility in this case as well. Here we probate a different interactive design by natural product hopping, molecular modelling, pharmacophore modelling, modification, and combination of the phytoconstituents present in different medicinal plants for developing a pharmacophore-guided good drug candidate for the variants of SARS-CoV-2 or Covid 19. In the modern era, these approaches are carried out at every level of development of scaffold queries, which are increasingly summarized from chemical structures. In this context, we report on a successfully designed drug-like candidate having a high-binding-affinity “compound SLP” by understanding the relationships between the compounds’ pharmacophores, scaffold functional groups, and biological activities beyond their individual applications that abide by Lipinski’s rule of five, Ghose rule, Veber rule etc. The new scaffold generated by altering the core of the known phyto-compounds holds a good predicted ADMET profile and is examined with iMODS server to check the molecular dynamics simulation with normal mode analysis (NMA). The scaffold’s three-dimensional (3D) structure yields a searchable natural product koenimbine from a conformer database having good ADMET property and high availability in spice *Murraya koenigii* leaves. *M. koenigii* leaves are easily available in the market, and might ensure the immunity, good health, and well-being of people if affected with any of the variants of Covid 19. The cell viability studies of koenimbine on murine colorectal carcinoma cell line (CT-26) showed no toxicity on normal mice lymphocyte cells (MLCs). The anticancer mechanism of koenimbine was displayed by its enhanced capacity to produce intercellular reactive oxygen species (ROS) in the colorectal carcinoma cell line.



INTRODUCTION

Before the discovery of modern medicines in the field of allopathy, in the ancient era, treating patients was an individual practice and doctors used to treat sick people with medicines obtained from nature, most of which were from medicinal plants or may be referred to as herbal drugs. Moreover, at that time, a huge amount of vegetation was sufficient to cater to their needs. It was believed that the efficiency of the plant medicines depends on the wholesome composition of the plant or a certain plant part. In the modern era, where isolation of phytoconstituents using chromatographic techniques and their structural elucidation are possible using nuclear magnetic resonance (NMR) and X-ray diffraction (XRD), one can easily find out the structure of molecules present in a medicinal

plant; also, with the development of biotechnology and biochemistry, the activity of a concerned structure can be easily studied. We aim to prepare a successful drug candidate that has the ability to bind at the active sites of the proteins and enzymes that help in the survival and replication of the Covid 19 virus by modifying the active ingredient using the

Received: July 2, 2022

Accepted: August 30, 2022

Published: September 10, 2022



scaffold architecture technique of the medicinal plant to make it better and easy to synthesize a drug molecule.

The active structures from medicinal plants have always paved the way to the development of drugs, and the objective of our study is to prepare a new drug candidate from raw plant secondary metabolites or active ingredients. We also consider other issues like the presence of heavy metals, α toxin residues, and specific pathogens while performing a molecular similarity search for an easily available food or spice having a similar natural product. As mentioned, computational advancements in biotechnology like the scaffold hopping method are applied to the new drug candidate and the method is capable of helping search engines toward producing new scaffolds that are likely to represent potent compounds with high therapeutic applications, which is a possibility in this case as well.

The Covid 19 virus has a spike glycoprotein that encourages the entry of human angiotensin-converting enzyme 2 (ACE2) receptor;¹ thus, if we can make a drug molecule that can bind to Spike-receptor-binding domain-ACE2 (Spike-RBD-ACE2) in a better way than the virus, then it can be seen as a good strategy to control the spread of infection. Along with these persuasions, a cysteine protease (3-chymotrypsin-like protease (3CLpro) or the main protease (M^{pro})) is found necessary for the viral life cycle of the Covid 19 virus.² Of functional importance is another protein as well that is responsible for the survival and replication of the virus; it is an enigmatic protein, an endo-ribonuclease that is highly needed for protein interference, called NSP15.³ Therefore, these three proteins were taken as fugitive targets for developing a potential drug candidate.

MATERIALS AND METHODS

Data Collection. Here the study was conducted by choosing compounds that are active ingredients of several medicinal plants, the native N3 ligand of 6LU7 protein, molnupiravir, and ivermectin⁴ as controls and chloroquine. The molecules belonging to the respective medicinal plant are individually considered for molecular docking study with all of the protein targets.

Molecular Docking. The *in silico* docking of the compounds, which is called the protein–ligand binding energy (ΔG) analysis, was performed using AutoDock Vina⁵ as an extension in UCSF Chimera.

The protein human ACE2-receptor, Nsp15 endo-ribonuclease, and M^{pro} were retrieved from RCSB Protein DataBank (PDB) (<http://www.rcsb.org/pdb>), PDB-ID 1R4L, 6VWW, and 6LU7 in PDB format. As per the docking protocol, removal of all water and solvent molecules, co-crystallized residues, and mirror chain (if any) was ensured using UCSF Chimera software. The next part is the protein structure preparation, which is also done in Chimera. The protein structures were prepared by assigning the hydrogen atoms, charges, and energy minimization using DockPrep tool. The charges were assigned as per the AM1-BCC method, which quickly and efficiently generates high-quality atomic charges for the protein, and the charges were computed using ANTECHAMBER algorithm.⁶ The energy minimization was performed using 500 steepest descent steps with 0.02 Å step size with an update interval of 10. The protein energy minimization of 6LU7 was further done with SwissPDB viewer⁷ as it contained a co-crystallized ligand. The target proteins after minimization of energy were then saved in PDB format for docking purpose.

All of the ligands used for the *in silico* interaction assays were mostly the medicinal plants' secondary metabolites and the structures that were present in PubChem were retrieved from there in SDF format along with the control of 6LU7, which is the N3 ligand, and 1R4L, which is Ivermectin, while others were directly drawn on ChemDraw; these drawn structures were copied to Chem3D pro, where their energy minimization was carried out using MM2 calculations (not for float structures). After that, they were saved in SDF format. Before performing the molecular docking of the ligand and protein, the ligands were optimized by addition of hydrogen and addition of charges using the Gasteiger algorithm.⁸ Energy minimization was performed using 1000 steepest descent steps with 0.02 Å step size with an update interval of 10 and then again saved in PDB format using the structure editing wizard of Chimera software, which is driven by the chemoinformatic principle of electronegativity equilibration; then the files were saved in PDB format. A grid box that assigns the binding region was chosen in such a way that it would cover the protein's active site for the hydrophobic surface of the concave region of the protein to fit in properly the hydrophobic surface of the ligand, giving the best binding score.

New molecules were designed by altering the architecture of the best-fit active phytoconstituents in two-dimensional (2D) format first using ChemDraw ultra-software, and then copying and pasting them in Chem3D pro to convert them to 3D SDF format after minimizing the energy of the molecules using MM2. The rest of the method of preparation of the molecules as ligands for docking is the same as above. For visualizing in different formats, we used the software Discovery studio and UCSF Chimera.

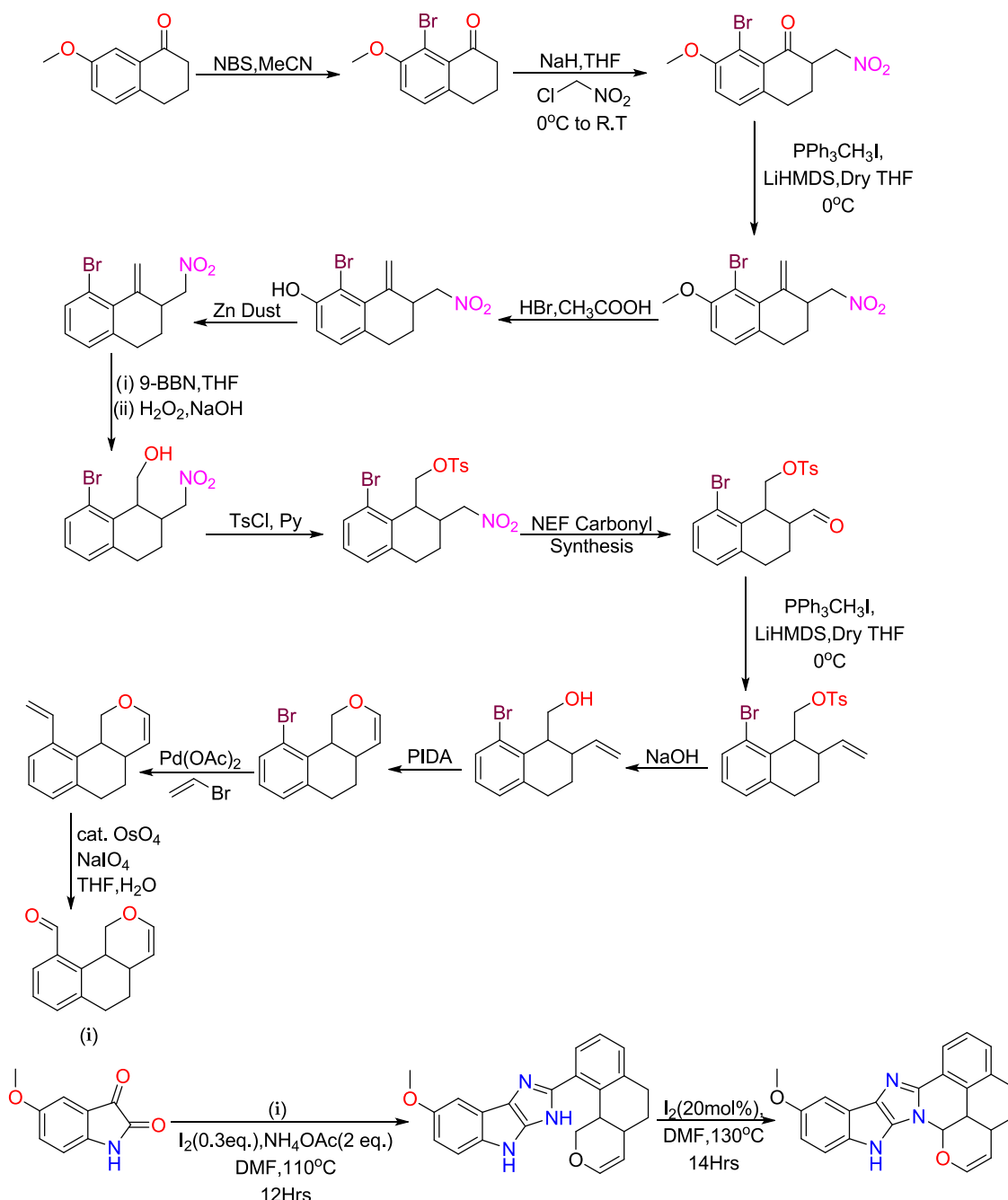
Scaffold Architecture. Scaffold architecture heir's new scaffolds utilize many aspects to replace active natural compounds with synthetic equivalents that are chemically easier to access. To this end, it is an attractive similarity-based computational approach typically attempted by pharmacophore-guided interactive designs capable of detecting compounds with different core structures having the same or enhanced activity and reliable absorption, distribution, metabolism, and excretion (ADME) properties. This method gently modulates the core structure of a natural product with different functional moieties such that the local or global similarity remains intact to a greater percentage while chemical and biological activities get enhanced.

Molecular Similarity Finding. Molecular similarity findings mainly depend on the similarity property principle, which means similar properties are shown by compounds that are similar chemically and structurally. In this study, the property chosen is predictive biological activity on the basis of the docking score with targeted proteins. Physicochemical descriptors like $\log P$, molecular weight, number of rotatable bonds etc., which are generally defined as mathematical models of chemical properties, are also taken into account. Similarity computed with compound SLP using ZINC software yields a significantly large number of compounds, most of which are either synthetic or semisynthetic.

Along with computational help, we also considered human perception and searched the secondary metabolites of medicinally important spices and foods.

All of the selected candidates were then subjected to docking analysis. The molecule that passed at least two control parameters and showed good ADME properties as predicted

Scheme 1. Schematic Presentation of the Probable Synthetic Pathway of the Molecule “SLP”



by SwissADME software was then chosen as the alternative of compound SLP.

ADMET Prediction. In silico ADME analysis was conducted to investigate the physicochemical properties of the potent hits, such as water solubility, lipophilicity, and pharmacokinetics, by using the website <http://www.swissadme.ch>,⁹ but the toxicity of these molecules cannot be investigated by using SwissADME, so the help of pk-CSM¹⁰—a pharmacokinetics server—was taken to predict the toxicity properties of the molecules with their SMILE (Simplified Molecule Input Line Entry Specification) profile.

Isolation of the Natural Product (Koenimbine). The leaves of *M. koenigii* Spreng. (Rutaceae) (100 g), commonly known as “Kurry patta” or “curry patta” in India, which is the only part that people consume, grow throughout India and also

in the Andaman Islands, collected from the local markets of West Bengal, India, were air dried and extracted with 1% ethylacetate in *n*-hexane in a Soxhlet apparatus for 72 h. The total extract was concentrated using a rotary evaporator and kept at room temperature for some time, then weighed, and found to have 1.22 g of a yellowish solid. This was dissolved in chloroform and chromatographed using a silica gel column and eluted with 2% ethylacetate in *n*-hexane.

The fraction obtained with 2% ethylacetate in *n*-hexane afforded a white solid, which after washing with *n*-hexane afforded 290 mg of pure koenimbine as a white buff solid; the structure was confirmed using ¹H-NMR. So the amount of koenimbine present in the leaves of *Murraya koenigii* is found to be 0.029%. The melting point was determined in open

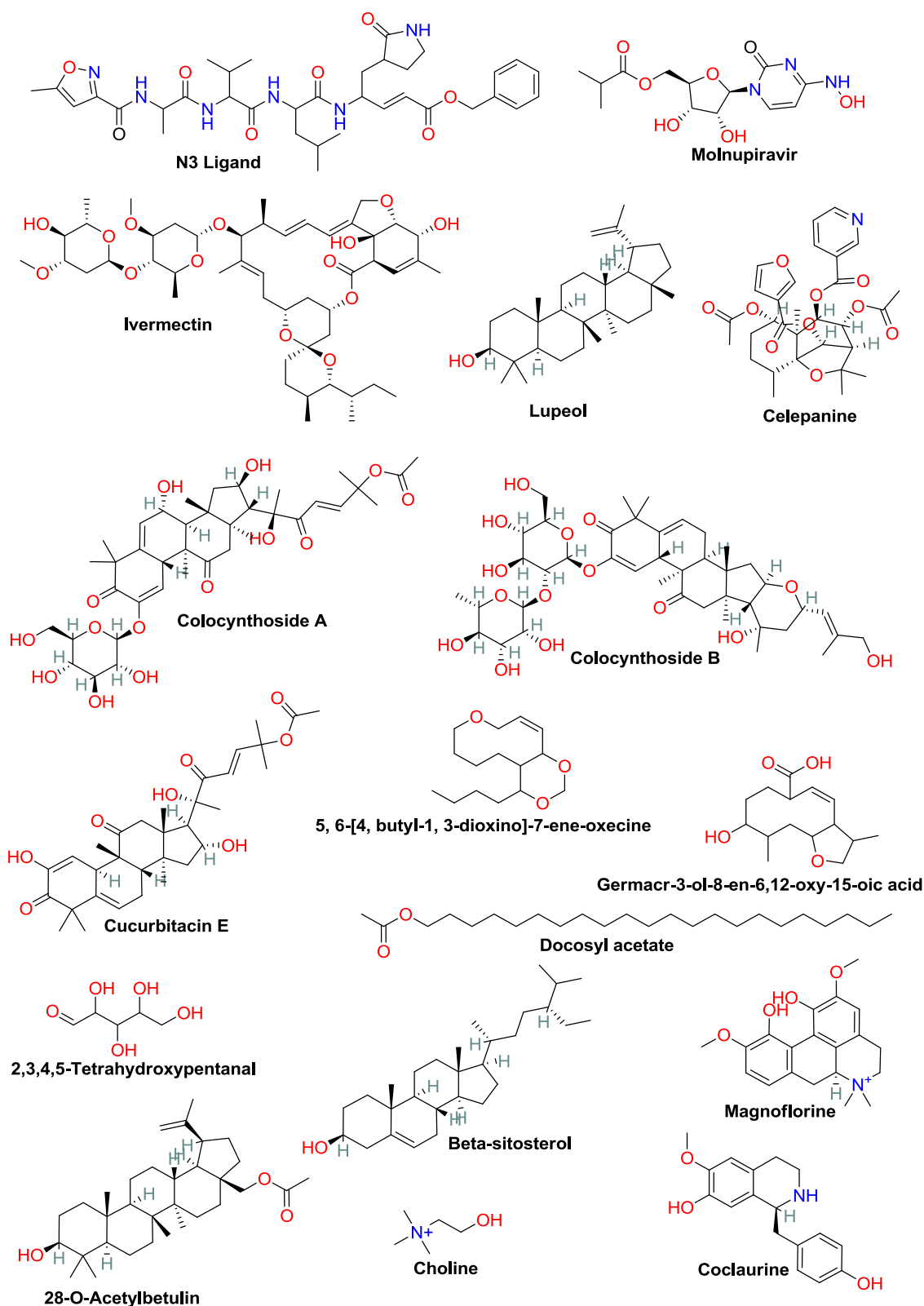


Figure 1. Structures of active ingredients of several medicinal plants from Table 1.

capillary tubes in a Köfler block apparatus and found to be 194.6 °C.

$^1\text{H-NMR}$ δ (CDCl_3): 1.49 (6H, s, H-2'a/H-2'b), 2.33(3H, s, H-3a), 3.91 (3H, s, H-6a), 5.71 (1H, d, $J = 10.0$ Hz, H-3'), 6.63 (1H, d, $J = 10.0$ Hz, H-4'), 6.97(1H, dd, $J = 10.0, 3.0$ Hz, H-7), 7.29 (1H, d, $J = 10.0$ Hz, H-8), 7.42 (1H, d, $J = 3.0$ Hz,

H-5), 7.63 (1H, s, H-4), 7.71 (1H, br.s, >NH). (Figure S1 in SI)

Probable Synthetic Pathway of Our Designed Molecule SLP. The designed molecule SLP can be synthesized from the easily available 7-methoxy- α -tetralone; bromination of the commercially available molecule is carried

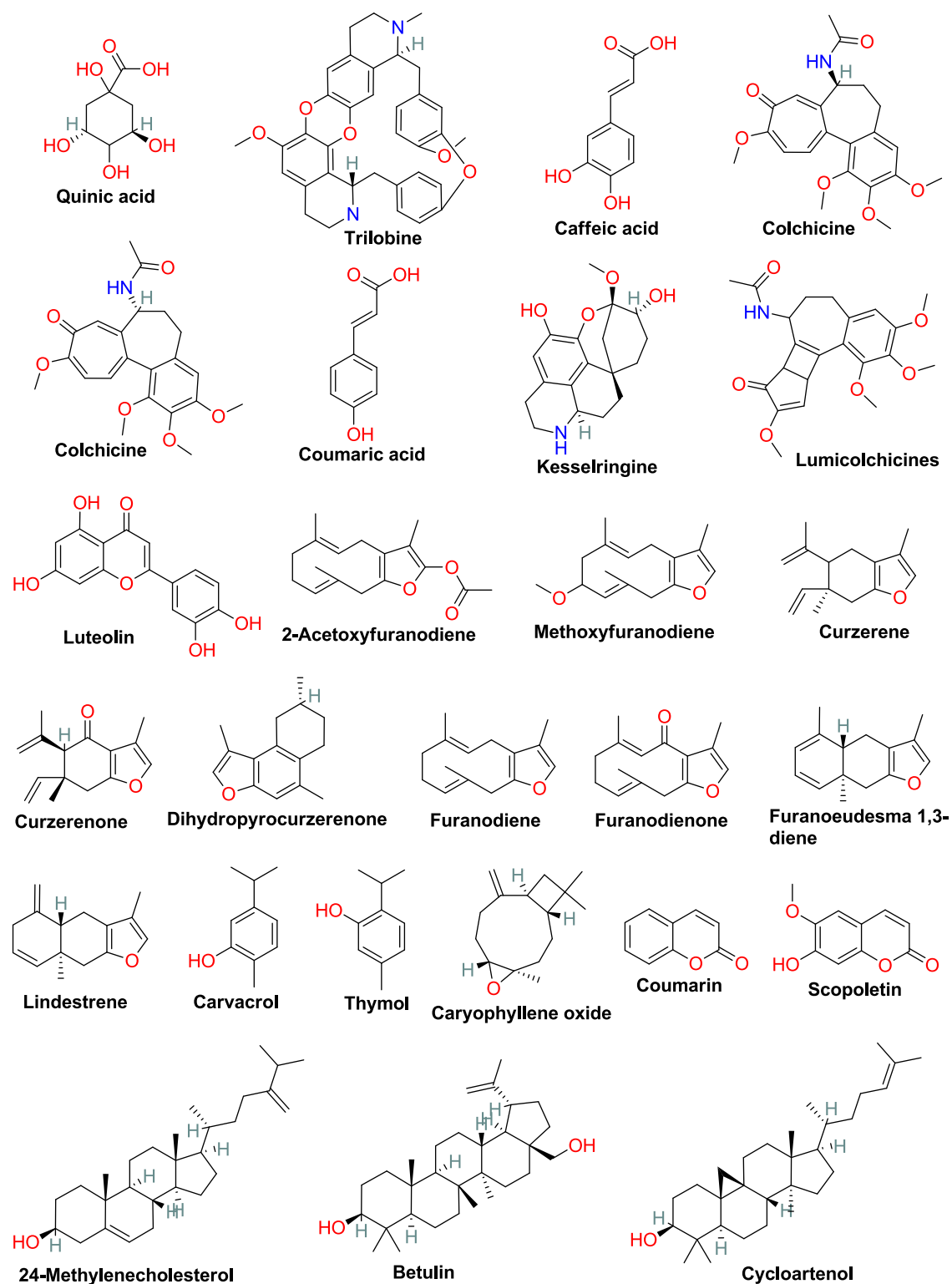


Figure 2. Structures of the active ingredients of several medicinal plants from Table 1.

out with NBS (*N*-bromosuccinamide) in acetone, followed by a series of steps (Scheme 1) to produce (i), which on treatment with 5-methoxy acetone in the presence of iodine and ammonium acetate with DMF solvent and heating to 110 °C for 12 h¹¹ produces our precursor molecule. Lastly, in the same reaction tube we added 20 mol % iodine and heated it at 130 °C for 14 h more.

Molecular Dynamics Simulation. Molecular dynamics simulation study of docked complexes plays a crucial part to validate the drug candidate and protein fit binding, molecular dynamics were carried out with iMODS server to explain the usual protein motion within the internal coordinates through normal mode analysis (NMA). iMODS¹² is a highly customizable and useful server and shows a number of levels which are coarse grained (CG). It predicts the dihedral coordinates of

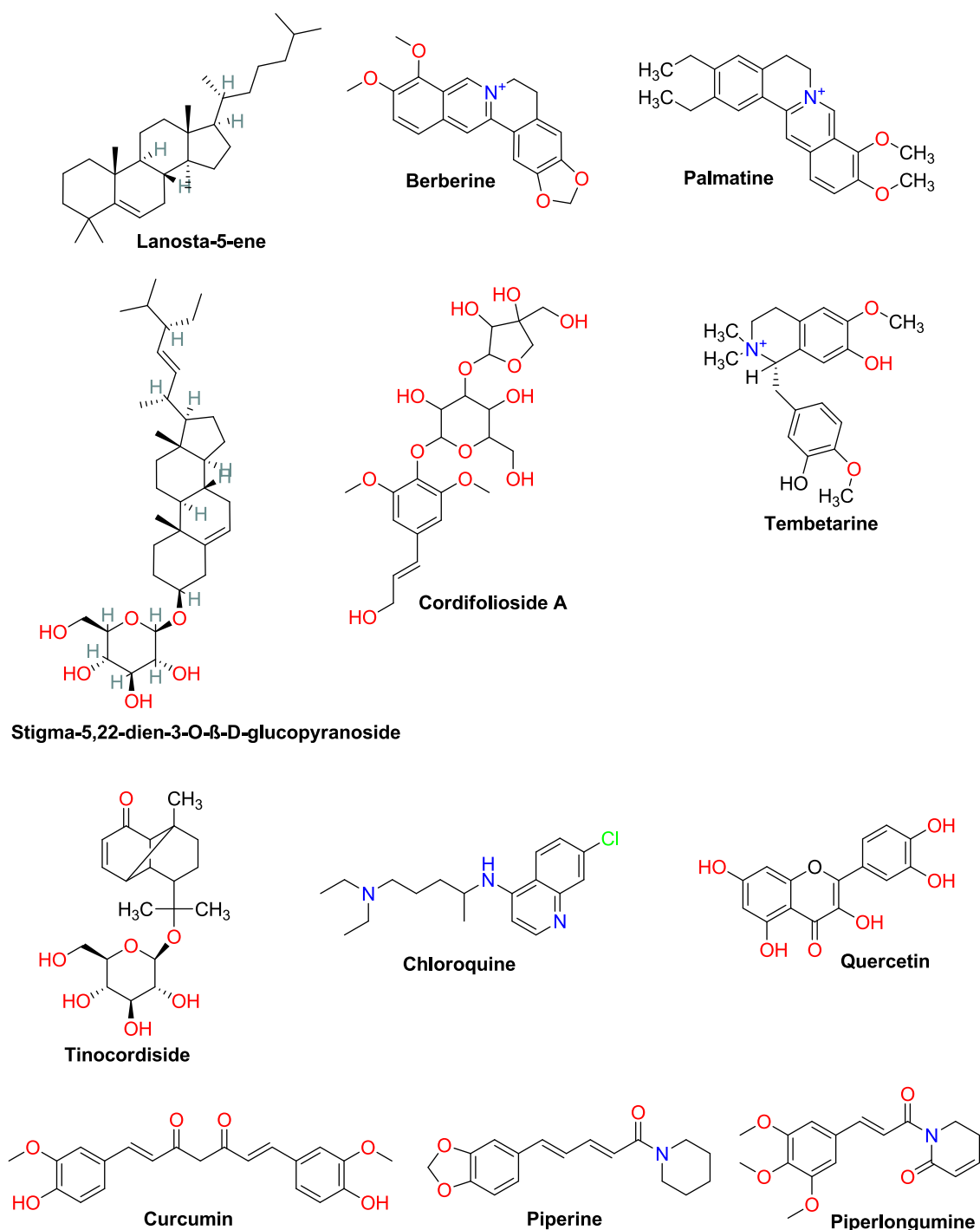


Figure 3. Structures of active ingredients of several medicinal plants and chloroquine from Table 1.

α atoms with large calculations of these big docked complexes. Furthermore, the B-factor is also predicted in the iMODS server along with structural deformability and determines eigenvalue.

Cell Viability Study of Koenimbine on Mice Lymphocyte Cells (MLCs) and the Murine Colorectal Carcinoma Cell Line (CT-26). The detailed methods and experiments of the cell viability study of koenimbine on MLCs and on CT-26 are given in the SI file.

Measurement of Intracellular ROS Generation. Intracellular ROS generation was measured using 2',7'-dichlorodihydrofluorescein diacetate (H₂DCFDA).¹³ CT-26 cells

were treated with Koenimbine at its IC₅₀ dose (20.47 μ g/mL) for 24 h. After that, Dulbecco's modified Eagle medium (DMEM) was discarded; the cells were washed with phosphate-buffered saline (PBS, pH 7.4) and incubated with H₂DCFDA (1 μ g/mL) for 30 min at 37 °C, then washed with PBS three times. Finally, oxidation of DCFH-DA to 2'-7'-dichlorofluorescein (DCF) was quantified using a Hitachi F-7000 fluorescence spectrophotometer at 485 nm (excitation) and 520 nm (emission). The image was recorded by fluorescence microscopy (LEICA DFC295, Germany). 5-Fluorouracil (5-FU) was used as positive control.

Table 1. Results of the Docking of Control Molecules, Secondary Metabolites, and Chloroquine

| name and structure | pubchem ID | docking score | | | name and structure | pubchem ID | docking score | | |
|---|------------|---------------|------|-------|--|------------|---------------|------|-------|
| | | 6LU7 | 6VWW | 1R4L | | | 6LU7 | 6VWW | 1R4L |
| control 1: N3 ligand | 146025593 | -6.9 | | | (25) 2-methoxyfuranodiene | 6325622 | -6.3 | -6.3 | -7.9 |
| control 2: molnupiravir | 145996610 | -6.8 | -7.0 | | (26) curzerene | 572766 | -5.7 | -6.1 | -7.1 |
| control 3: ivermectin | 6321424 | | | -10.9 | (27) curzerenone | 3081930 | -6.1 | -7 | -7.3 |
| (1) lupeol | 259846 | -7.3 | -7.5 | -9.8 | (28) dihydroprocuzerenone | 91734838 | -6.3 | -7 | -8.1 |
| (2) celepanine | 442518 | -7.1 | -7.4 | -8.7 | (29) furanodiene | 9601230 | -5.9 | -7.1 | -7.4 |
| (3) 5,6-[4-butyl-1,3-dioxino]-7-ene-oxecine | | -5.9 | -5.5 | -6.9 | (30) furanodienone | 6442374 | -6.3 | -6.4 | -7.7 |
| (4) choline | 305 | -3.7 | -3.8 | -3.5 | (31) furanoedesma 1,3-diene | 643237 | -6.6 | -7.1 | -8.2 |
| (5) colocynthoside A | 16216752 | -8.1 | -8.3 | -10.3 | (32) lindestrene | 12311270 | -6.4 | -7.7 | -8.3 |
| (6) colocynthoside B | 16216649 | -7.3 | -8.1 | -10.2 | (33) 24-methylenecholesterol | 921113 | -7.9 | -8.1 | -9.6 |
| (7) cucurbitacin E | 5281319 | -7.4 | -8.4 | -10 | (34) betulin | 72326 | -7.3 | -7.5 | -9.5 |
| (8) docosyl acetate | 69969 | -4.4 | -3.9 | -5.6 | (35) carvacrol | 10364 | -5.2 | -6 | -6 |
| (9) germacr-3-ol-8-en-6,12-oxy-15-oic acid | | -6.6 | -6.3 | -8 | (36) caryophyllene oxide | 1742210 | -6.3 | -6.1 | -7.1 |
| (10) 2,3,4,5-tetrahydroxypentanal | 854 | -4.5 | -5.2 | -5.6 | (37) coumarin | 323 | -5.6 | -6.4 | -6.4 |
| (11) 28-O-acetylbetulin | 14038495 | -7.8 | -8.2 | -9 | (38) cycloartenol | 92110 | -7.4 | -8.3 | -10.4 |
| (12) β -sitosterol | 222284 | -7.5 | -8.1 | -9.4 | (39) lanosta-5-ene | 123204535 | -6.9 | -7.8 | -9.9 |
| (13) coclaurine | 160487 | -7.5 | -7.7 | -8.5 | (40) scopoletin | 5280460 | -5.7 | -6.4 | -7 |
| (14) magnoflorine | 73337 | -6.9 | -7.7 | -10 | (41) stigma-5,22dien-3-O- β -D-glucopyranoside | 6602508 | -6.9 | -9 | -9.8 |
| (15) quinic acid | 6508 | -5.4 | -6.4 | -6.6 | (42) thymol | 6989 | -4.9 | -6.6 | -6.2 |
| (16) trilobine | 169007 | -8.4 | -9.3 | -10.5 | (43) berberine | 2353 | -7.5 | -7.7 | -8.2 |
| (17) caffeic acid | 689043 | -6 | -6.7 | -6.5 | (44) cordifolioside A | 75111036 | -7.1 | -7.1 | -8.4 |
| (18) colchicine | 6167 | -6.2 | -6.9 | -7.8 | (45) palmatine | 19009 | -7 | -7 | -8 |
| (19) colchimine | | -6.6 | -7.5 | -8.4 | (46) tembetarine | 167718 | -6.4 | -7.1 | -8.6 |
| (20) coumaric acid | 637542 | -6 | -6.2 | -6.1 | (47) tinocordiside | 177384 | -7.6 | -8.2 | -9.7 |
| (21) kesselringine | 76967674 | -7.3 | -7.9 | -8.6 | (48) chloroquine | 2719 | -5.7 | -6.1 | -7 |
| (22) lumicolchicines | 244898 | -6.9 | -6.7 | -7.5 | (49) quercetin | 5280343 | -7.2 | -8 | -8.4 |
| (23) luteolin | 5280445 | -7.4 | -8.3 | -8.6 | (50) curcumin | 969516 | -6.7 | -8.4 | -9.3 |
| (24) 2-acetoxifyuranodiene | 91748044 | -7 | -7.3 | -8.4 | (51) piperine | 638024 | -6.6 | -7.8 | -8.3 |
| | | | | | (52) piperlongumine | 637858 | -6.1 | -7.1 | -8.1 |

RESULTS

Docking Results. Docking Studies. The protein–ligand binding interactions between the targeted proteins PDB-ID 6LU7, 6VWW, and 1R4L and the ligands, which are mainly phytoconstituents of medicinal plants, were found out using molecular docking. The calculations reveal the highest free energy change for these interactions as $\Delta G = -8.4$ kcal/mol for trilobine for Protein M^{Pro} 6LU7 inside a grid box of $-10.75 \text{ \AA} \times 12.33 \text{ \AA} \times 68.84 \text{ \AA}$ with size $30 \text{ \AA} \times 30 \text{ \AA} \times 30 \text{ \AA}$ along the x -, y -, and z - axes. For Protein Nsp15 endo-ribonuclease 6VWW, predicted calculations reveal the free energy change for these interactions as $\Delta G = -9.3$ kcal/mol for trilobine inside a grid box of $-67 \text{ \AA} \times 30 \text{ \AA} \times 26 \text{ \AA}$ with size $30 \text{ \AA} \times 30 \text{ \AA} \times 30 \text{ \AA}$ along the x -, y -, and z - axes. For Protein Human ACE2-receptor (A-Chain) 1R4L, predicted calculations reveal the free energy change for these interactions as $\Delta G = -10.5$ kcal/mol for trilobine inside a grid box of $38 \text{ \AA} \times 2 \text{ \AA} \times 26 \text{ \AA}$ with size $71 \text{ \AA} \times 56 \text{ \AA} \times 59 \text{ \AA}$ along the x -, y -, and z -axes (Figures 1–3 and Table 1).

Scaffold Architecture. Trilobine showed the best binding among all other phytoconstituents chosen in this case. It binds better than the control molnupiravir and N3 ligand. but less effective than the control Ivermectin, so we architected a new design by altering the structure of trilobine so that we can make a new and improved drug candidate for Covid 19 (Figure 4).

The newly designed molecule SLP showed better protein–ligand binding interactions with the targeted proteins 6LU7

(inside a grid box of $-10.75 \text{ \AA} \times 12.33 \text{ \AA} \times 68.84 \text{ \AA}$ with size $30 \text{ \AA} \times 30 \text{ \AA} \times 30 \text{ \AA}$ along the x -, y -, and z -axes), 6VWW (inside a grid box of $-67 \text{ \AA} \times 30 \text{ \AA} \times 26 \text{ \AA}$ with size $30 \text{ \AA} \times 30 \text{ \AA} \times 30 \text{ \AA}$ along the x -, y -, and z -axes), and 1R4L (inside a grid box of $38 \text{ \AA} \times 2 \text{ \AA} \times 26 \text{ \AA}$ with size $71 \text{ \AA} \times 56 \text{ \AA} \times 59 \text{ \AA}$ along the x -, y -, and z - axes) than the control molecules, as evidenced from its docking scores given in Table 2, and it can easily be synthesized in a lab or industry at a low cost (Figures 5–7).

Molecular Similarity Finding. However, time is an important factor, and as we know, the time requirement is quite high to bring a new drug molecule into the market since it has to pass lots of parameter tests, which are highly necessary. In order to meet the rush, we discovered a molecule that showed high molecular, structural, chemical, biological, and local similarities like the number of rotatable bonds, H-bond acceptors, and H-bond donors etc. to the known spice *M. koenigii* Spreng. (Rutaceae) and can be consumed every day since it has much availability; it also showed better binding than controls 1 and 2 (evidenced in Table 3) and thus can be used to combat the virus causing Covid 19 (Figure 8).

Koenimbine is a natural product and has good molecular similarity to our designed compound SLP. It is available in the spice *M. koenigii*, which along with koenimbine has a lot of other active components as well; so it can be a good choice of food on the table during Covid 19 disease (Figures 9–11).

Cell Viability Study of Koenimbine on Mice Lymphocyte Cells (MLCs) and the Murine Colorectal Carcinoma Cell Line (CT-26). The cell viabilities of MLCs and CT-26

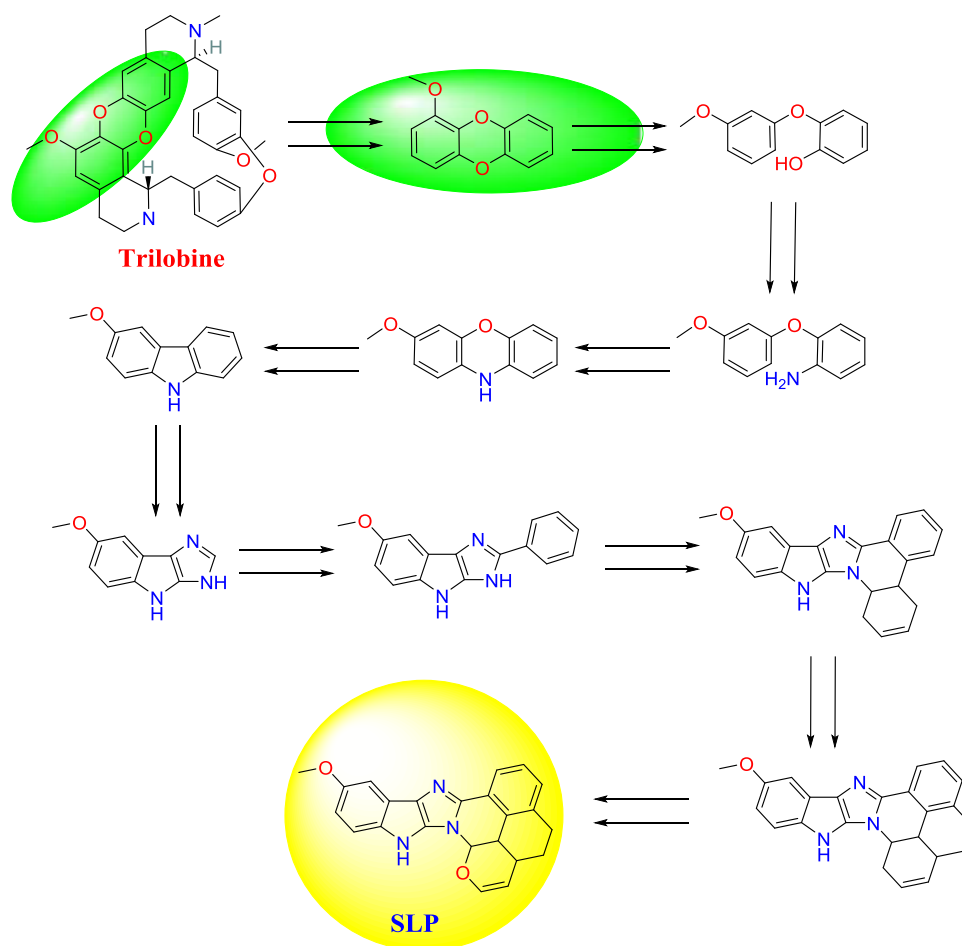


Figure 4. Scaffold architecture of SLP from trilobine.

Table 2. Docking Score of the SLP Molecule

| name and structure | pubchem ID | docking score | | |
|--------------------|------------|---------------|------|-------|
| | | 6LU7 | 6VWW | 1R4L |
| SLP | | -8.5 | -9.9 | -11.4 |

cells were studied by MTT assay. The results showed that koenimbine significantly inhibited CT-26 cells' viability in a concentration-dependent manner as compared to the CT-26 control group (Figure 12). As the concentration was increased, the growth of cells seemed to be decreased and the IC_{50} value

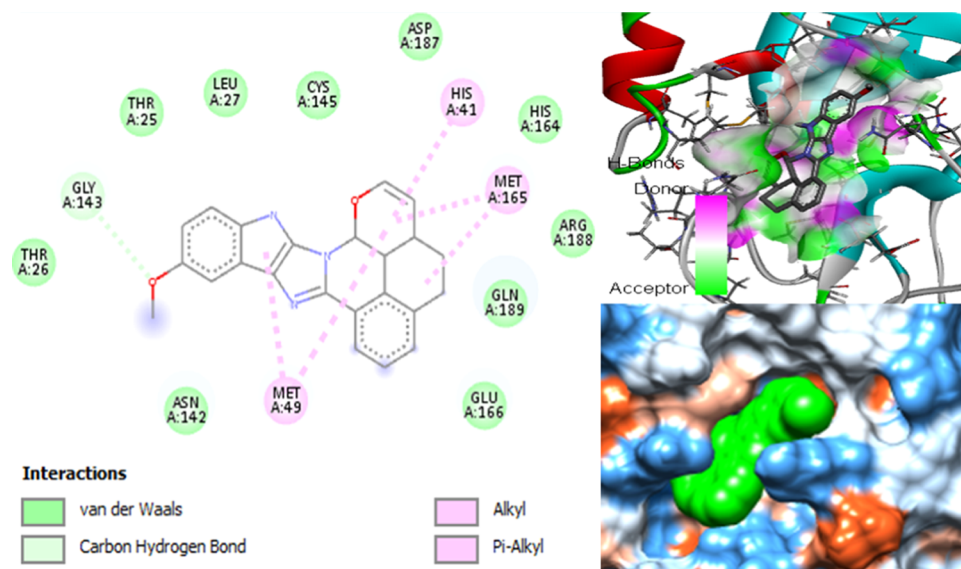


Figure 5. Docking poses of SLP with 6LU7.

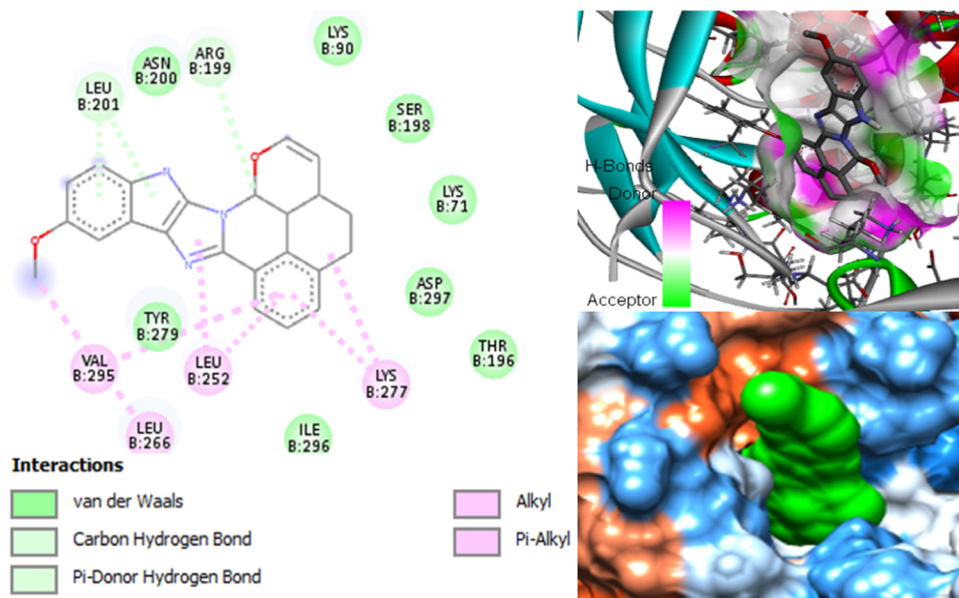


Figure 6. Docking poses of SLP with 6VWW.

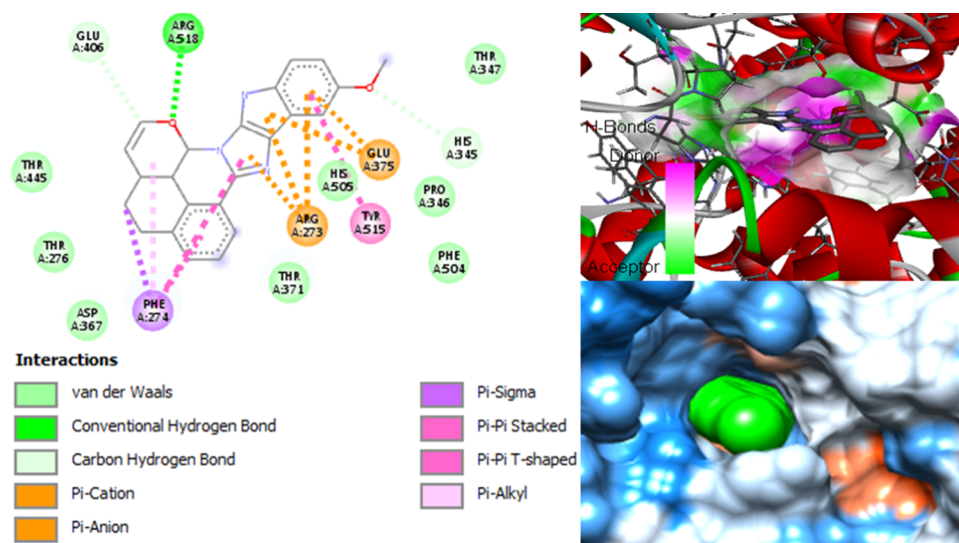


Figure 7. Docking poses of SLP with 1R4L.

Table 3. Results of the Docking of Koenimbine

| name and structure | pubchem ID | docking score | | |
|--------------------|------------|---------------|------|------|
| | | 6LU7 | 6VWW | 1R4L |
| koenimbine | 97487 | -7.1 | -7.9 | -9.3 |

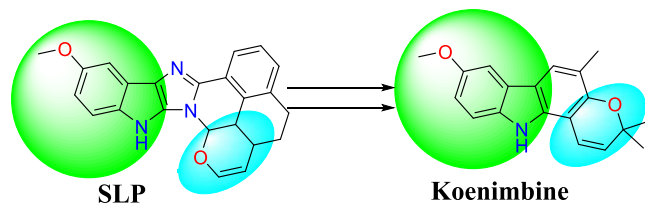


Figure 8. Molecular, structural, chemical, biological, and local similarities of koenimbine with SLP.

of koenimbine was found to be $20.47 \pm 2.48 \mu\text{g/mL}$. However, the IC_{50} value of 5-FU was $14.57 \pm 3.08 \mu\text{g/mL}$, which is

significantly ($##p < 0.01$) different from that of koenimbine. This result indicates the potent cytotoxic effect of koenimbine in CT-26 cells.

On the other hand, koenimbine did not alter MLC cells' viability significantly up to $25 \mu\text{g/mL}$, and at the concentration of $100 \mu\text{g/mL}$, the viability of MLC cells was significantly ($***p < 0.001$) reduced to 52% as compared to the control group. Meanwhile, in the koenimbine-treated group, the viability of MLC cells was found to be 69% at the concentration of $50 \mu\text{g/mL}$, which is significantly ($##p < 0.01$) different as compared to the 5-FU-treated group (Figure 13). From the above results, koenimbine was found to be nontoxic for MLC cells up to $50 \mu\text{g/mL}$ with more than 50% cell viability.

These results suggested that koenimbine exhibited significant cytotoxicity against CT-26, but at the same time, koenimbine was found to be nontoxic for MLC cells. In conclusion, koenimbine could be used as a potent anticancer agent for colorectal cancer therapy.

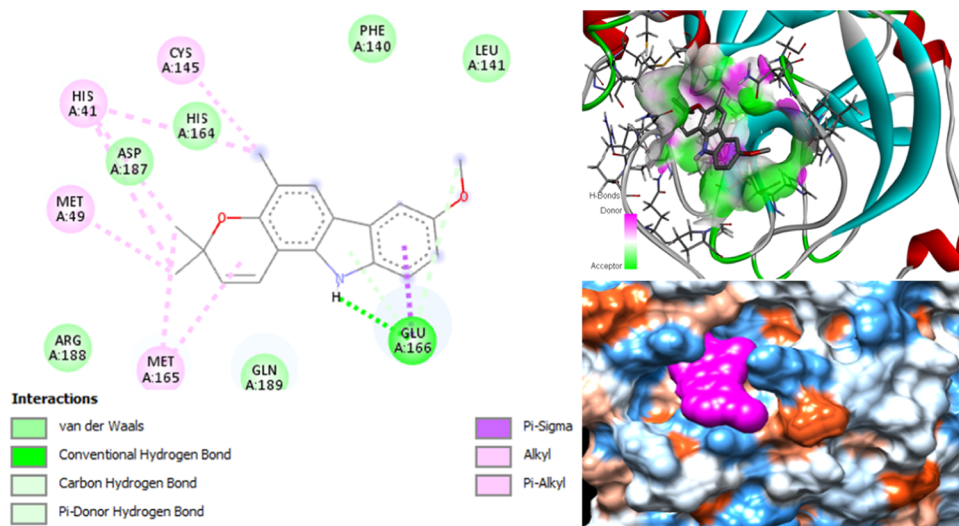


Figure 9. Docking poses of koenimbine with 6LU7.

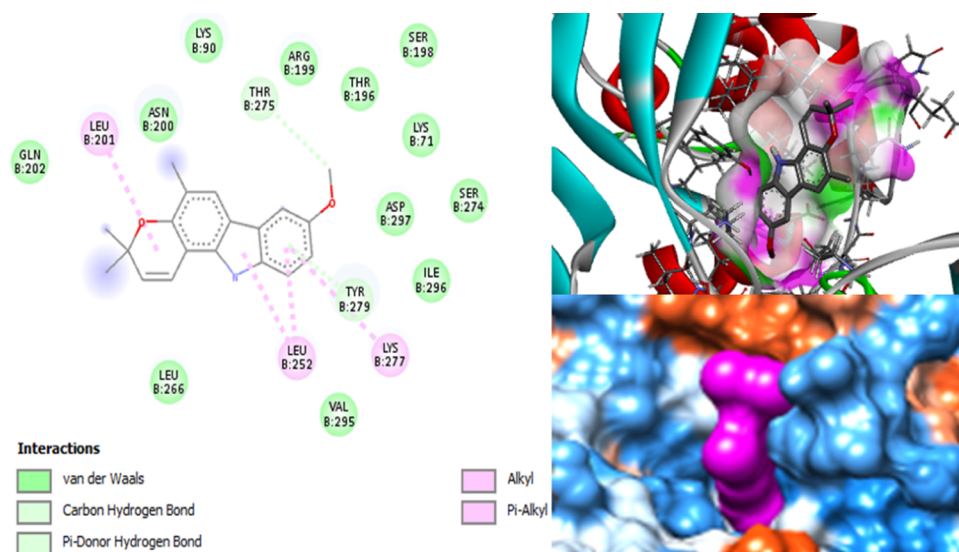


Figure 10. Docking poses of koenimbine with 6VWW.

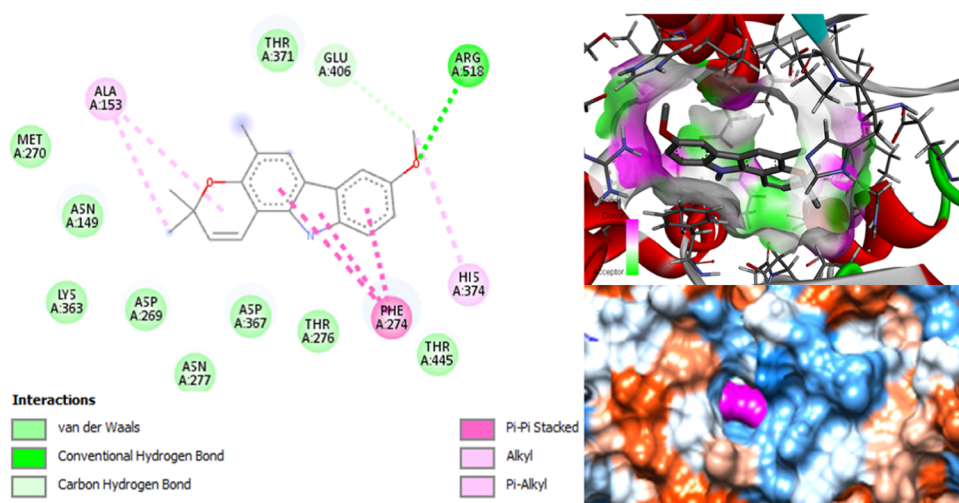


Figure 11. Docking poses of koenimbine with 1R4L.

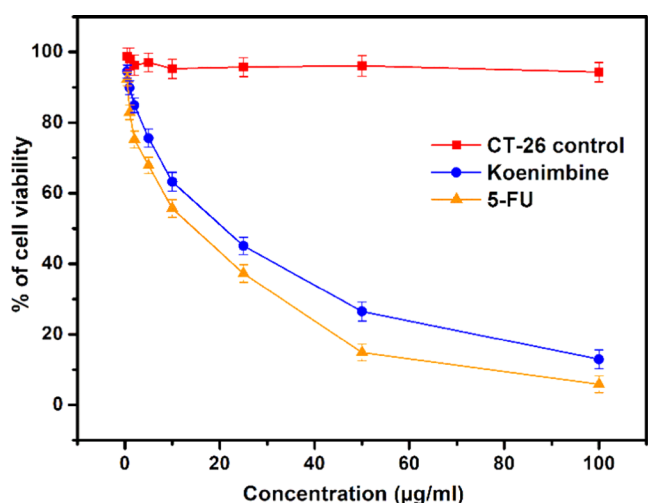


Figure 12. Cytotoxicity study of koenimbine on CT-26 cells by MTT assay. CT-26 cells were treated with different concentrations (0.5–100 µg/mL) of koenimbine for 24 h in a CO₂ incubator. The IC₅₀ value of koenimbine and 5-FU were found to be 20.47 ± 2.48 and 14.57 ± 3.08 µg/mL, respectively. 5-FU was used in the experiment as a standard drug. The values are expressed as the mean ± SEM of three independent experiments.

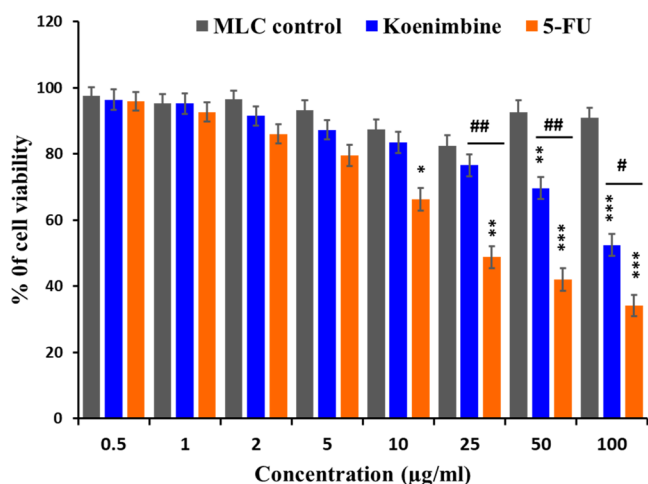


Figure 13. Cell viability study of mice lymphocyte cells (MLCs) by MTT assay. MLC cells were treated with different concentrations (0.5–100 µg/mL) of koenimbine and 5-FU for 24 h. The values are expressed as the mean ± SEM of three independent experiments (* $p < 0.05$, ** $p < 0.01$, *** $p < 0.001$ compared with the control. # $p < 0.05$, ## $p < 0.01$ compared with 5-FU).

Intracellular ROS Generation in CT-26 Colorectal Carcinoma Cells. The results showed that the fluorescence intensity of DCF was significantly ($P < 0.001$) increased compared to the CT-26 control group after the treatment with koenimbine, and this was similar to the effect of the positive control 5-FU (Figure 14). This may be due to the conversion of H₂DCFDA to the highly fluorescent 2',7'-dichlorofluorescein (DCF) in the presence of excessive free radicals.¹³ The fluorescence microscopic image showed a bright green color, which indicates the enhanced intracellular ROS generation (Figure 15). Reactive oxygen species (ROS) are the natural active byproduct containing unpaired valence electrons, which are mainly generated by mitochondrial respiration.¹³ The excessive levels of ROS generation generally damage the DNA,

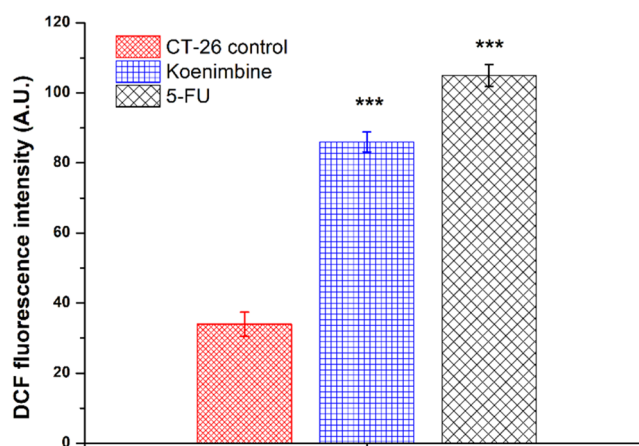


Figure 14. Measurement of the dichlorofluorescein (DCF) fluorescence intensity induced by koenimbine in CT-26 colorectal carcinoma cells. Values are expressed as the means ± SEM of three experiments; *** $p < 0.001$; comparison was done with the CT-26 control group.

proteins, and lipids, and ultimately cause cell death.¹⁴ The ROS-based therapeutic strategy is used in recent times to kill cancer cells by increasing the intracellular ROS generation.¹⁴ Here, koenimbine showed its CT-26 cell killing property possibly through the enhanced intracellular ROS generation in CT-26 cells (Figures 14 and 15).

Molecular Dynamics Simulation. Molecular dynamics simulation study of docked complexes plays a crucial part in validating the secondary metabolites and protein fit binding, which can be shown as a comparison in the normal mode of the prepared protein analysis dynamics. In this case, dynamics study of the essential protein docked complexes was applied to the selected number of normal modes of the prepared protein to determine their mobility, rigidness, and stability through the iMODS server. In this case, the study comprises the binding dynamics of the three docked complexes of compound SLP with the three targeted proteins. B-factor values feathered the amplitude relative to the displacements of atoms around the state of equilibrium; this was also witnessed with the help of NMA, which can be considered an equivalent of or close to RMS (Figure 16).

DISCUSSION

In our approach, we choose a pool of secondary metabolites from known medicinal plants of high importance to bind with three proteins, Spike-RBD-ACE2, 3-chymotrypsin-like protease (3CLpro) or the main protease (M^{pro}), and endoribonuclease protein interference, called NSP15. From the docking results it was found that trilobine showed the best binding among all other phytoconstituents chosen in this case. It binds better than the control molnupiravir and N3 ligand, but is less effective than the control ivermectin. We aspired to design a molecule that will bind with the target proteins better than their respective control molecules; for this, we architected the structure of trilobine by taking the zone that showed the highest interactions and altering it with new motifs as shown in Figure 4, so that it can become an improved drug candidate for Covid 19, as evidenced from its docking score given in Table 2. The newly architected molecule SLP showed better binding than trilobine and all other controls as well. The predicted ADME property of SLP is also better than that of trilobine and

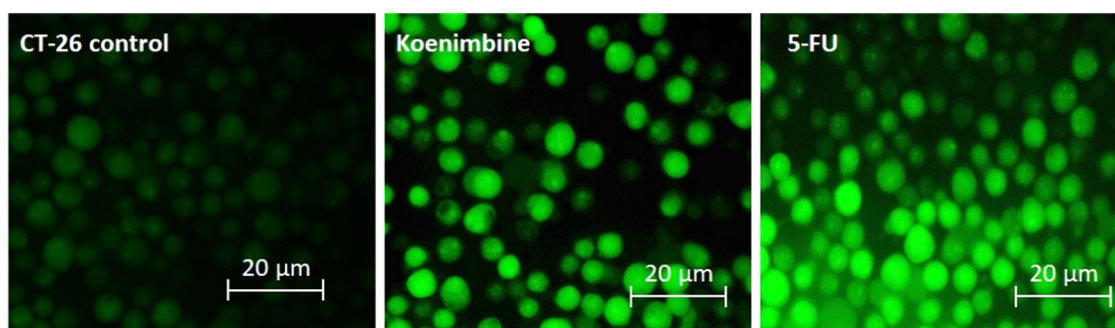


Figure 15. Fluorescence microscopic image of reactive oxygen species (ROS) generation in CT-26 cells using H_2DCFDA stain after the treatment with koenimbine. Scale bar: 20 μm .

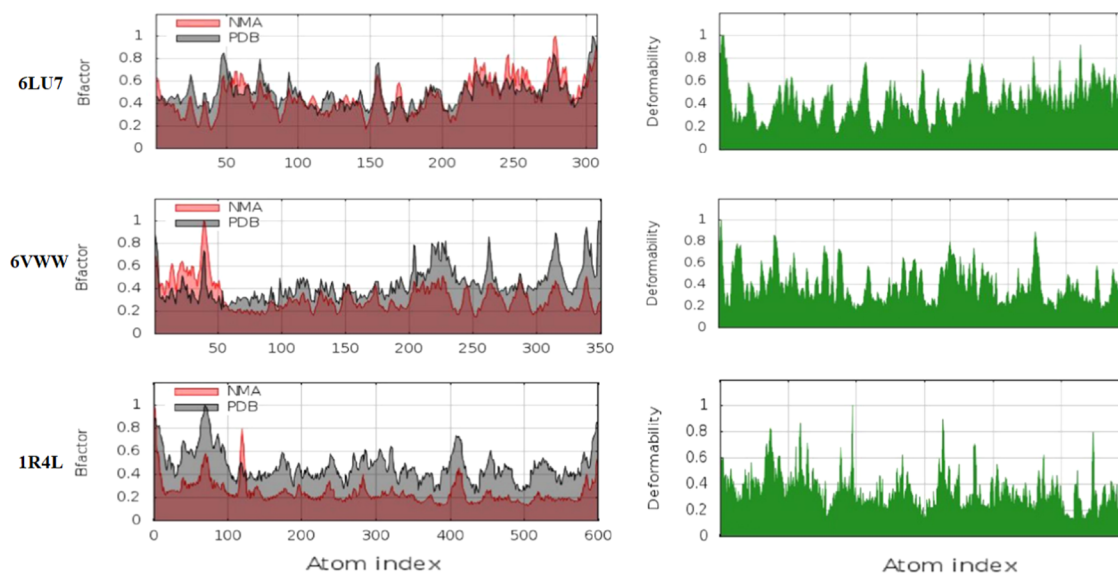
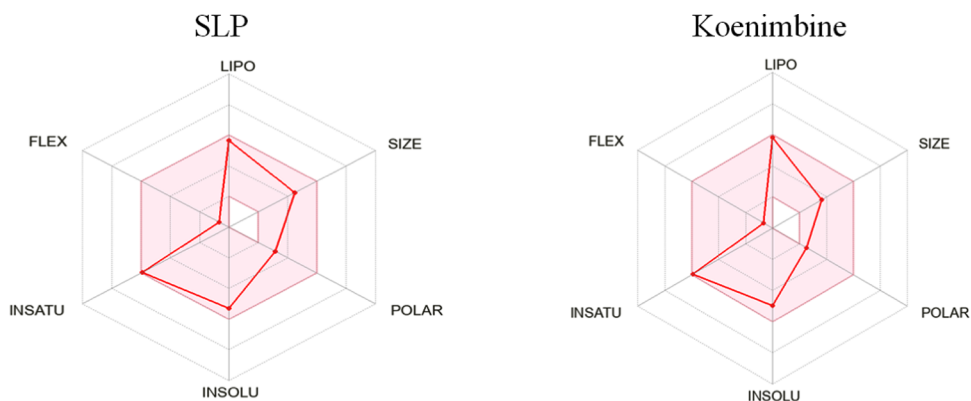


Figure 16. B-Factor and deformability of SLP with 6LU7, 6VWW, and 1R4L.

Table 4. Bio-Radar Similarity to Oral Bioavailability



it has passed all the parameters of drug likeness like Lipinski rule of five, Veber, Ghose, Egan, and Muegge rule. It has a good gastrointestinal (GI) absorption as well and can be orally admissible; all of these are found using the prediction software SwissADME. This process of scaffold architecture is used for the first time as it is totally based on human perception since a lot of molecules are to be designed in order to reach a desired molecule for multipurpose use.

Previous approaches using computer-aided methods to reach a new lead molecule are scaffold hopping,^{15–19} structure-based

drug discovery,^{20,21} ligand-based drug discovery,^{22,23} fragment-based drug discovery,^{24,25} and vector-based search,²⁶ but these methods concentrate on fragments of existing drug molecules or natural products²⁷ of high medicinal value; these connect the chemical structure and biological activity by understanding their SAR (structure activity relationship).^{28,29} All of these methods proceed through either single-point modification or a certain moiety modification. In addition, vector-based methods help to change the core structure with suitable bioisosteric scaffold fragments; the morphine rule on the other hand

Table 5. Bar Diagram of the Binding Strength Comparison between Controls, Trilobine, SLP, and Koenimbine

COMPARATIVE NEGATIVE FREE ENERGY CHANGE(-ΔG)

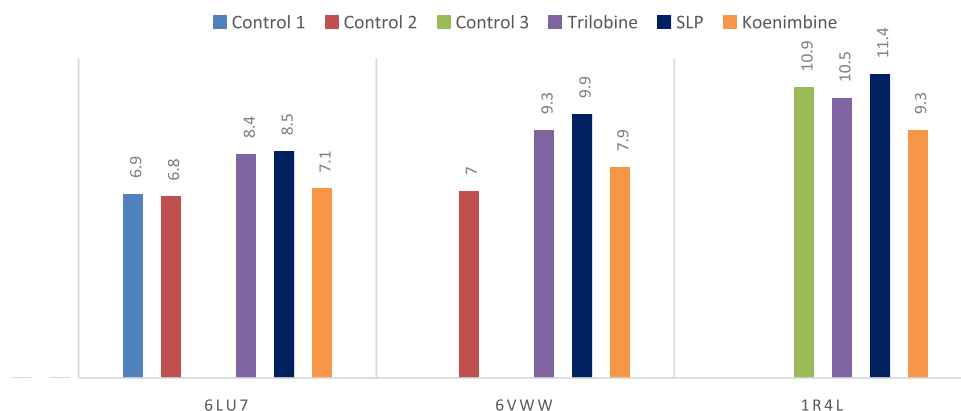


Table 6. Results of ADME Prediction and Comparison

| SLP | | koenimbine | |
|--------------------------------------|---|--|---|
| Physicochemical Properties of "SLP" | | Physicochemical Properties of "Koenimbine" | |
| formula | C ₂₃ H ₁₉ N ₃ O ₂ | formula | C ₁₉ H ₁₉ NO ₂ |
| molecular weight | 369.42 g/mol | molecular weight | 293.36 g/mol |
| num. heavy atoms | 28 | num. heavy atoms | 22 |
| num. arom. heavy atoms | 18 | num. arom. heavy atoms | 13 |
| fraction Csp ³ | 0.26 | fraction Csp ³ | 0.26 |
| num. rotatable bonds | 1 | num. rotatable bonds | 1 |
| num. H-bond acceptors | 3 | num. H-bond acceptors | 2 |
| num. H-bond donors | 1 | num. H-bond donors | 1 |
| molar refractivity | 108.21 | molar refractivity | 91.38 |
| TPSA | 52.07 Å ² | TPSA | 34.25 Å ² |
| Lipophilicity of "SLP" | | Lipophilicity of "Koenimbine" | |
| log P _{o/w} (iLOGP) | 2.93 | log P _{o/w} (iLOGP) | 3.19 |
| log P _{o/w} (XLOGP3) | 4.37 | log P _{o/w} (XLOGP3) | 4.65 |
| log P _{o/w} (WLOGP) | 4.57 | log P _{o/w} (WLOGP) | 4.71 |
| log P _{o/w} (MLOGP) | 3.47 | log P _{o/w} (MLOGP) | 3.24 |
| log P _{o/w} (SILICOS-IT) | 3.61 | log P _{o/w} (SILICOS-IT) | 4.96 |
| consensus log P _{o/w} | 3.79 | consensus log P _{o/w} | 4.15 |
| Pharmacokinetics of "SLP" | | Pharmacokinetics of "Koenimbine" | |
| GI absorption | high | GI absorption | high |
| BBB permeant | yes | BBB permeant | yes |
| P-gp substrate | yes | P-gp substrate | yes |
| CYP1A2 inhibitor | yes | CYP1A2 inhibitor | yes |
| CYP2C19 inhibitor | yes | CYP2C19 inhibitor | yes |
| CYP2C9 inhibitor | no | CYP2C9 inhibitor | yes |
| CYP2D6 inhibitor | no | CYP2D6 inhibitor | yes |
| CYP3A4 inhibitor | no | CYP3A4 inhibitor | no |
| log K _p (skin permeation) | -5.45 cm/s | log K _p (skin permeation) | -4.79 cm/s |
| Drug Likeness of "SLP" | | Drug Likeness of "Koenimbine" | |
| Lipinski | yes; 0 violation | Lipinski | yes; 0 violation |
| Ghose | yes | Ghose | yes |
| Veber | yes | Veber | yes |
| Egan | yes | Egan | yes |
| Muegge | yes | Muegge | yes |
| bioavailability score | 0.55 | bioavailability score | 0.55 |

identifies the structural features responsible for its biological activity and modifies it to an easily synthesizable molecule. All of these methods yield quite a number of compounds, which

results in an immense amount of time requirement; so, to reduce this extra time, computational binding is tested. This method starts from a readily available drug candidate or drug

molecule and does not consider directly the drug likeness, lead likeness, or oral viability of the designed compounds. This is a considerable difference from our applied method.

But, establishing a new molecule as a drug for a specific disease takes a long time since it has to pass lots of parameter tests, which are highly necessary. Thus, we thought of repurposing³⁰ a natural product along with its source plant, which has high availability in nature. In order to cater to our need, we discovered a molecule named koenimbine, which showed high molecular, structural, chemical, biological, and local similarities,³¹ like the number of rotatable bonds, H-bond acceptors, H-bond donors, drug likeness, bio-radar similarity etc., to the known spice *M. koenigii* Spreng. (Rutaceae) that can be consumed every day since it has much availability and it also showed better binding than controls 1 and 2 (evidenced in Table 3) and thus can be used to combat the virus causing Covid 19 (Table 4).

To place koenimbine for the drug screen test, we performed the cell viability assay, which infers the overall health of cells and measures their survival rates in the presence of the molecule used for treatment. Here we took colorectal cancer as the disease of concern due to the unavailability of Covid 19-infected cell samples and resources. Koenimbine from *M. koenigii* Spreng. (Rutaceae) significantly inhibited CT-26 cells' viability in a concentration-dependent manner as compared to the CT-26 control group (Figure 12). Koenimbine exhibited significant cytotoxicity against CT-26, showed CT-26 cell killing property possibly through the enhanced intracellular ROS generation in CT-26 cells (Figure 12), and at the same time, was found to be nontoxic for MLC cells (Tables 5 and 6).

CONCLUSIONS

The search for a new drug candidate by the scaffold architecture technique inspired from the structures of secondary metabolites of several medicinal plants via modification, addition, and deletion of groups backed by docking studies and other scientific approaches opened up a new territory in the field of drug design and discovery. The ethno-pharmacological, ethno-botanical, and pharmacological importance of medicinal plants, which led us to examine their active principles as cure for SARS-CoV-2 infection, helped in this study to architect our new drug candidate SLP with a good structural backbone and theoretically biological role. Compound SLP, according to bioinformatics studies, can act as an inhibitor of human ACE2-receptor (A-Chain), protein Nsp15 endo-ribonuclease (B-chain), and SARS-CoV-2 main protease, and acts better than all of the control molecules considered, as shown in Table 4. The synthesis of SLP and its in vitro and in vivo activity evaluation against all of the said proteins could be useful in clinical assays. However, bringing a new molecule into the market as a drug takes a long time and also we have to keep in mind not to destroy our vegetation of medicinal plants. Therefore, we found out a similar molecule, koenimbine, present in a known spice with high availability in nature, *M. koenigii* Spreng. (Rutaceae); it holds a better docking score than control 1 and control 2 and also showed anticancer property against colorectal cancer. The IC₅₀ value of koenimbine evidenced from the cell viability study on mice lymphocyte cells (MLCs) and murine colorectal carcinoma cell lines (CT-26) was found to be 20.47 ± 2.48 μg/mL. Overall, as SLP will not be available, one can use *M. koenigii* Spreng. (Rutaceae) as it contains a high amount of koenimbine to

prevent and cure any future variants of Covid 19, and it could also be used as a potent anticancer drug for colorectal cancer therapy, for which the mechanism was established through the ROS generation experiment.

ASSOCIATED CONTENT

Supporting Information

The Supporting Information is available free of charge at <https://pubs.acs.org/doi/10.1021/acsomega.2c04051>.

Supporting information includes ADMET properties of SLP and Koenimbine from pK-CSM server and ¹H NMR spectra of Koenimbine (PDF)

AUTHOR INFORMATION

Corresponding Author

Malay Dolai – Department of Chemistry, Prabhat Kumar College, Purba Medinipur 721404 West Bengal, India; orcid.org/0000-0001-7697-3376; Email: dolaimalay@yahoo.in

Authors

Sourav Pakrashi – Department of Chemistry, Prabhat Kumar College, Purba Medinipur 721404 West Bengal, India

Prakash K. Mandal – Department of Chemistry, University of Calcutta, Kolkata 700003 West Bengal, India

Surya Kanta Dey – Biochemistry, Molecular Endocrinology, and Reproductive Physiology Laboratory, Department of Human Physiology, Vidyasagar University, Midnapore 721102 West Bengal, India

Sujata Maiti Choudhury – Biochemistry, Molecular Endocrinology, and Reproductive Physiology Laboratory, Department of Human Physiology, Vidyasagar University, Midnapore 721102 West Bengal, India

Fatmah Ali Alasmary – Department of Chemistry, College of Science, King Saud University, Riyadh 11451, Saudi Arabia

Amani Salem Almalki – Department of Chemistry, College of Science, King Saud University, Riyadh 11451, Saudi Arabia

Md Ataul Islam – Division of Pharmacy and optometry, School of Health Sciences, Faculty of Biology, Medicine and Health, University of Manchester, Manchester M13 9PL, United Kingdom; orcid.org/0000-0001-6286-6262

Complete contact information is available at:

<https://pubs.acs.org/doi/10.1021/acsomega.2c04051>

Notes

The authors declare no competing financial interest.

ACKNOWLEDGMENTS

M.D. thanks Dr. Gautam Dutta, Dept of Physiology, Prabhat Kumar College, Contai, for his constant support for carrying out the biological application. The authors acknowledge the financial support received from the I-STEM program funded by the Office of the Principal Scientific Adviser to the Government of India to carry out the research work in Prabhat Kumar College, Contai facilities listed on and booked through the I-STEM web portal. F.A.A. and A.S.A. are thankful to the researcher supporting project (RSP-2021/259), King Saud University, Riyadh, Saudi Arabia.

REFERENCES

(1) Zhang, H.; Penninger, J. M.; Li, Y.; Zhong, N.; Slutsky, A. S. Angiotensin-Converting Enzyme 2 (ACE2) as a SARS-CoV-2

Receptor: Molecular Mechanisms and Potential Therapeutic Target. *Intensive Care Med.* **2020**, *46*, 586–590.

(2) Jin, Z.; Du, X.; Xu, Y.; Deng, Y.; Liu, M.; Zhao, Y.; et al. Structure of M pro from SARS-CoV-2 and Discovery of Its Inhibitors. *Nature* **2020**, *582*, 289–293.

(3) Kim, Y.; Jedrzejczak, R.; Maltseva, N. I.; Wilamowski, M.; Endres, M.; Godzik, A.; Michalska, K.; Joachimiak, A. Crystal Structure of Nsp15 Endoribonuclease NendoU from SARS-CoV-2. *Protein Sci.* **2020**, *29*, 1596–1605.

(4) Eweas, A. F.; Alhossary, A. A.; Abdel-Moneim, A. S. Molecular Docking Reveals Ivermectin and Remdesivir as Potential Repurposed Drugs Against SARS-CoV-2. *Front. Microbiol.* **2021**, *11*, No. 3602.

(5) Allouche, A. R. Gabedit — A Graphical User Interface for Computational Chemistry Softwares. *J. Comput. Chem.* **2012**, *32*, 174–182.

(6) Wang, J.; Wang, W.; Kollman, P. A.; Case, D. A. Antechamber, An Accessory Software Package For Molecular Mechanical Calculations. *J. Am. Chem. Soc.* **2001**, *123*, 2222–2231.

(7) Guex, N.; Peitsch, M. C. SWISS-MODEL and the Swiss-PdbViewer: An Environment for Comparative Protein Modeling. *Electrophoresis* **1997**, *18*, 2714–2723.

(8) Gasteiger, J.; Jochum, C. An Algorithm for the Perception of Synthetically Important Rings. *J. Chem. Inf. Comput. Sci.* **1979**, *19*, 43–48.

(9) Daina, A.; Michielin, O.; Zoete, V. SwissADME: a free web tool to evaluate pharmacokinetics, drug-likeness and medicinal chemistry friendliness of small molecules. *Sci. Rep.* **2017**, *7*, No. 42717.

(10) Pires, D. E. V.; Blundell, T. L.; Ascher, D. B. PkCSM: Predicting Small-Molecule Pharmacokinetic and Toxicity Properties Using Graph-Based Signatures. *J. Med. Chem.* **2015**, *58*, 4066–4072.

(11) Adhikary, S.; Majumder, L.; Pakrashi, S.; Srinath, R.; Mukherjee, K.; Mandal, C.; Banerji, B. Polysubstituted Imidazoles as LysoTracker Molecules: Their Synthesis via Iodine/H₂O and Cell-Imaging Studies. *ACS Omega* **2020**, *5*, 14394–14407.

(12) López-Blanco, J. R.; Aliaga, J. I.; Quintana-Ortí, E. S.; Chacón, P. IMODS: Internal Coordinates Normal Mode Analysis Server. *Nucleic Acids Res.* **2014**, *42*, W271–W276.

(13) Pradhan, A.; Bepari, M.; Maity, P.; Roy, S. S.; Roy, S.; Choudhury, S. M. Gold nanoparticles from indole-3-carbinol exhibit cytotoxic, genotoxic and antineoplastic effects through the induction of apoptosis. *RSC Adv.* **2016**, *6*, 56435–56449.

(14) Niu, B.; Liao, K.; Zhou, Y.; Wen, T.; Quan, G.; Pan, X.; Wu, C. Application of glutathione depletion in cancer therapy: Enhanced ROS-based therapy, ferroptosis, and chemotherapy. *Biomaterials* **2021**, *277*, No. 121110.

(15) Schneider, G.; Neidhart, W.; Giller, T.; Schmid, G. “Scaffold-Hopping” by Topological Pharmacophore Search: A Contribution to Virtual Screening. *Angew. Chem., Int. Ed.* **1999**, *38*, 2894–2896.

(16) Sun, H.; Tawa, G.; Wallqvist, A. Classification of Scaffold-Hopping Approaches. *Drug Discovery Today* **2012**, *17*, 310–324.

(17) Hu, Y.; Stumpfe, D.; Bajorath, J. Computational Exploration of Molecular Scaffolds in Medicinal Chemistry. *J. Med. Chem.* **2016**, *59*, 4062–4076.

(18) Hu, Y.; Stumpfe, D.; Bajorath, J. Recent Advances in Scaffold Hopping. *J. Med. Chem.* **2017**, *60*, 1238–1246.

(19) Koch, G. Medicinal Chemistry. *Chimia* **2017**, *71*, 643.

(20) Batool, M.; Ahmad, B.; Choi, S. A Structure-Based Drug Discovery Paradigm. *Int. J. Mol. Sci.* **2019**, *20*, No. 2783.

(21) Meng, X.-Y.; Zhang, H.-X.; Mezei, M.; Cui, M. Molecular Docking: A Powerful Approach for Structure-Based Drug Discovery. *Curr. Comput.-Aided Drug Des.* **2011**, *7*, 146–157.

(22) Bottgoni, G. Protein-ligand docking. *Front. Biosci.* **2011**, *16*, 2289–2306.

(23) Baskin, I. I. The Power of Deep Learning to Ligand-Based Novel Drug Discovery. *Expert Opin. Drug Discovery* **2020**, *15*, 755–764.

(24) Erlanson, D. A.; McDowell, R. S.; O'Brien, T. Fragment-Based Drug Discovery. *J. Med. Chem.* **2004**, *47*, 3463–3482.

(25) Murray, C. W.; Rees, D. C. The Rise of Fragment-Based Drug Discovery. *Nat. Chem.* **2009**, *1*, 187–192.

(26) Lauri, G.; Bartlett, P. A. CAVEAT: A Program to Facilitate the Design of Organic Molecules. *J. Comput.-Aided Mol. Des.* **1994**, *8*, 51–66.

(27) Kawamura, S.; Unno, Y.; Hirokawa, T.; Asai, A.; Arisawa, M.; Shuto, S. Rational Hopping of a Peptidic Scaffold into Non-Peptidic Scaffolds: Structurally Novel Potent Proteasome Inhibitors Derived from a Natural Product, Belactosin A. *Chem. Commun.* **2014**, *50*, 2445–2447.

(28) Yeh, J. Y.; Coumar, M. S.; Horng, J. T.; Shiao, H. Y.; Kuo, F. M.; Lee, H. L.; Chen, I. C.; Chang, C. W.; Tang, W. F.; Tseng, S. N.; Chen, C. J.; Shih, S. R.; Hsu, J. T. A.; Liao, C. C.; Chao, Y. S.; Hsieh, H. P. Anti-Influenza Drug Discovery: Structure-Activity Relationship and Mechanistic Insight into Novel Angelicin Derivatives. *J. Med. Chem.* **2010**, *53*, 1519–1533.

(29) Jamieson, A. G.; Boutard, N.; Sabatino, D.; Lubell, W. D. Peptide Scanning for Studying Structure-Activity Relationships in Drug Discovery. *Chem. Biol. Drug Des.* **2013**, *81*, 148–165.

(30) Auld, D. Rethinking Molecular Similarity: Comparing Compounds on the Basis of Biological Activity: Commentary. *Assay Drug Dev. Technol.* **2012**, *10*, 309–310.

(31) Maggiora, G.; Vogt, M.; Stumpfe, D.; Bajorath, J. Molecular Similarity in Medicinal Chemistry. *J. Med. Chem.* **2014**, *57*, 3186–3204.